SLAC-PUB-12095
September, 2006

Optical effects of the wake fields*

S. Heifets, S. Novokhatski, D. Teytelman
Stanford Linear Accelerator Center, Stanford University, Stanford, CA 94309, USA

Abstract

We discuss optical effects of the wake fields: synchronous phase and bunch length variation along the train of bunches, effect of the wakes on the tune and on the Twiss parameters.

1 Introduction

The wake fields generated by the beam in the beam pipe are recognized as the cause of the numerous beam instabilities [1]. Less attention was given to optical effects of the wakes which do not lead to bunch instability but may be important for beam dynamics and luminosity of a collider. It is important to estimate such effects. First of all, quite often a machine is studied and optimized at low currents while tune and Twiss parameters can vary with current and the optics at collision can differ from the optimized optics at low current. Therefore optimization of optics at low currents does not necessarily means optimization of the luminosity of a collider. More than that, in the multi-bunch machines the wake affects different bunches differently. The second reason is given by the need for study of the machine impedance. Usually, there are three main contributions to the impedance budget: the rf cavities, resistive wall (RW) impedance, and the impedance generated by small vacuum components of the ring such as bellows, beam position monitors, tapers, masks, vacuum ports, etc. The first two components give long-range wakes and are responsible for coupled-bunch (CB) instabilities, longitudinal and transverse, respectively. Usually, they are well known from cold measurements of rf cavities, 3D simulations of EM fields, and geometry of the machine. It is much more difficult to determine the impedance of vacuum components both numerically and experimentally. Therefore, analysis of the current dependence of the tunes, synchronous phase, and of the bunch length is crucial

Submitted to 3rd Workshop On Super Flavor Factory Based On Linear Collider Technology (Super B III), 14-16 June 2006, Menlo Park, CA

*Work supported in part by Department of Energy contract DE-AC02-76SF00515

to extract impedance parameters from the measurements. In the paper we analyze some of the current dependent effects. Results are obtained for PEP-II low energy ring (LER) but may be relevant for other projects such as Super-B-factories [3] and the ILC project. In the Appendix we discuss the relation between the rms of a single bunch and the bunch in a train of bunches.

2 Variation of the bunch length and synchronous phase along the train of bunches

Experimental measurements of the bunch length was carried out comparing two signals from a BPM at two frequencies. The bunch frequency envelope for a bunch with rms length $\sigma_l \simeq 1$ cm starts to roll off at frequency $\simeq 5$ GHz. The frequencies of the signals were chosen to be on the slope of the envelope. In this case, the ratio of amplitudes of two signals provides information on the bunch length. Results of measurements in the LER of PEP-II depicted in Fig. (1) show variation of the bunch length along the train of 1722 bunches.

This variation is caused by the gap in the train of bunches [2]. The gap in the LER matches the ion gap in the electron high-energy-ring (HER) and is needed also for the beam abort due to the finite rise time of a kicker. In the last runs, the machine is filled with 1722 bunches with the bunch separation $2\lambda_{RF}$ and 2% gap. One can expect that a small gap with the length s_g would generate transients of the rf voltage of the order of

$$1 - e^{-\frac{\omega_{rf} s_g}{2Q_L c}}. \tag{1}$$

Effect, actually, is larger. A small 2% gap gives substantial variation of the wake affecting different bunches and, as result, of the synchronous phase along the train. The variation of the synchronous phase contributes to variation of the slope of the rf voltage and, therefore, causes variation of the synchronous frequency f_s. An example of such variation calculated for LER parameters at the total rf voltage $V_{tot} = 4.5$ MV is shown in Fig. (2). The variations of the synchronous phase for the PEP-II with large beam loading is due, mostly, to the fundamental mode of the rf cavities. Other rf HOMs give smaller contribution to this effect.

2.1 Bunch length measurements

Transients variation of the rf phase and the synchrotron frequency of the bunch centroid along the train affect the rms length of a bunch, see discussion in the Appendix. Results of calculations are shown in Fig. (3), where bottom plot gives variation of the bunch length caused by the transients of the rf voltage, and the upper plot includes both the transients and the bunch lengthening due to potential well distortion (PWD). The amplitude and the period of the variation depend on the beam current I_B and increase with I_B. Both,

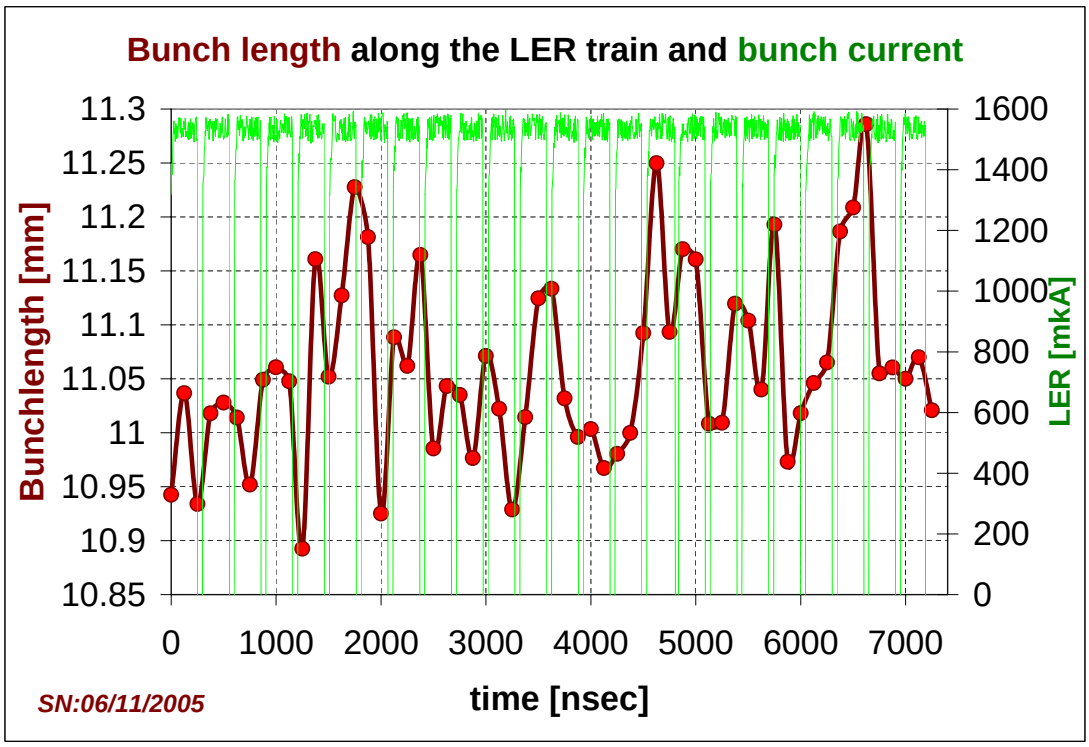

Figure 1: Variation of the bunch length along the train (red) and the bunch current (yellow), (S. Novokhatski).

the amplitude and the modulation frequency, depend on the detuning of the cavity and the effect is maximum when the detuning is equal to the revolution frequency which takes place for PEP-II parameters at, approximately, $I_b = 2.5$ A.

The bunch length measured without gating on individual bunches gives the average rms over the whole train. The averaging over the train rms gives current dependence shown in Fig. (4). Calculations are based on the estimate of the LER impedance [5] which gives inductance of the vacuum components $L_{ind} = 80$ nH. The number is, certainly, only an estimate. The real inductance is, probably, higher partially due to vacuum components added after the estimate was carried out. The fit gives

$$\frac{d\sigma_l}{I_B} = 0.83\, mm/mA. \tag{2}$$

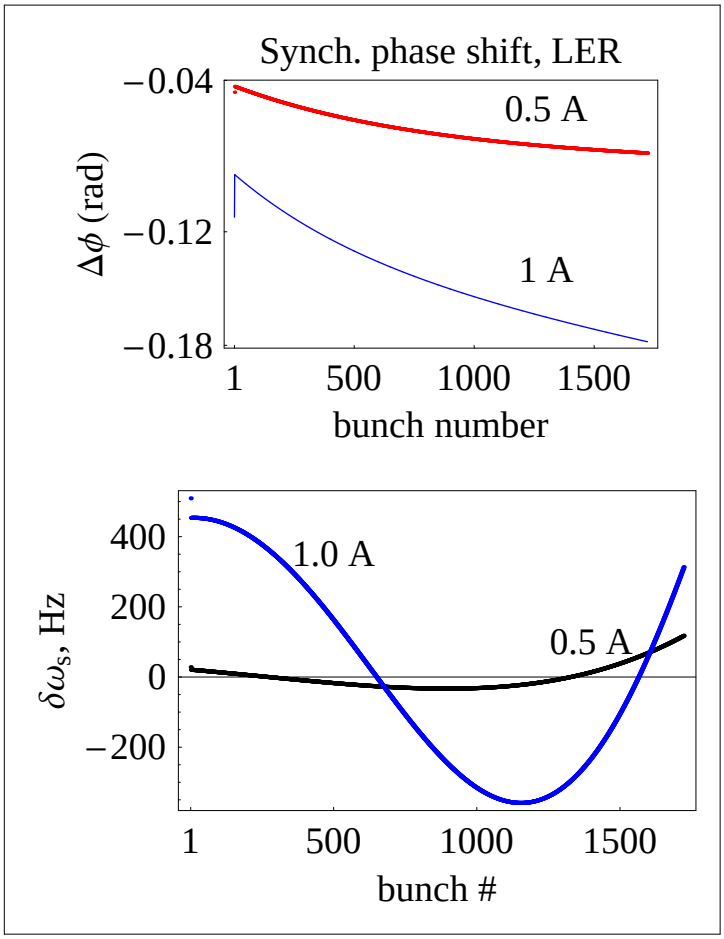

Figure 2: Synchronous phase (top) and synchrotron frequency (bottom) along the train caused by the ion gap for the beam current 0.5 and 1.0 Amp.

The measurement in PEP-II give close numbers: the streak-camera measurements give $d\sigma/dI = 0.8$ mm/mA while the bunch length extracted from the bunch spectrum gives somewhat higher value, $d\sigma/dI = 1.45$ mm/mA. It is encouraging that calculations give result close to the measurements although it is not clear whether the remaining discrepancy is due to underestimated inductance in calculations or due to errors of measurements.

It is worth to make the following remarks. Generally, the bunch length for a single bunch in the ring σ_1 and the average bunch length in a train of bunches σ are different for the same rf voltage and the bunch current. It can be shown (see Appendix) that, in the linear over the beam current approximation, they are related:

$$\sigma_1^2 = (\frac{\hat{\omega}_s}{\omega_{s,0}})^2 \, \sigma^2, \tag{3}$$

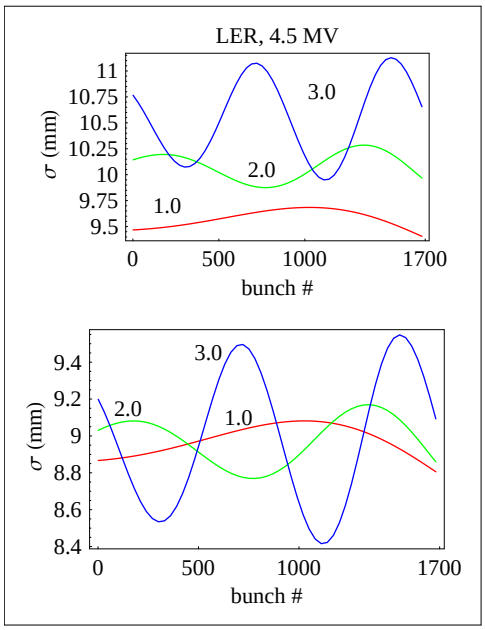

Figure 3: Calculated variation of the bunch length along the train for LER $V = 4.5MV$ and the beam currents (indicated in the figure) $I_B = 1.0, 2.0$ and $I_B = 3.0$ Amp. Bottom plot: results of only gap transients. Upper plot: variation due to the gap transients and the PWD. Note increase of the variation with the detuning.

where $\omega_{s,0}$ is the zero-current synchrotron frequency and $\hat{\omega}_s$

$$\hat{\omega}_s^2 = \omega_{s,0}^2 + \lambda\sigma_0\omega_{s0}^2 \langle W[\sigma_0(x' - x)]\rangle. \tag{4}$$

More discussion is given in the Appendix.

It is worth noting, that ω_s measured by different methods can give different results. The best method of determining ω_s is by measuring the frequency of the second synchrotron side-band of the rf frequency which is less affected by the feed-back system. The actual situation is quite complicated because each bunch centroid oscillates with different frequencies. Fortunately, the split of CB frequencies and is not large.

As it is well known, the head-tail instability can give the shift of the synchro-betatron sideband but should not be included in Haissinski calculations because the shift is result of the $x - z$ correlation in a bunch and does not change the longitudinal oscillations of the bunch centroid. The $2\omega_s$ sideband give better measurements of ω_s but, actually, there are two $2\omega_s$ lines in the spectrum. One is due to the nonlinearity of the oscillations of the bunch centroids, another one is the coherent quadrupole longitudinal CB oscillations related to the oscillations of the bunch profile. These frequencies are, generally, different.

Eqs. (3), (4) can be verified experimentally. Fig. (5) show two lines: one, the measurements of the bunch length in a train of bunches as function of beam current.

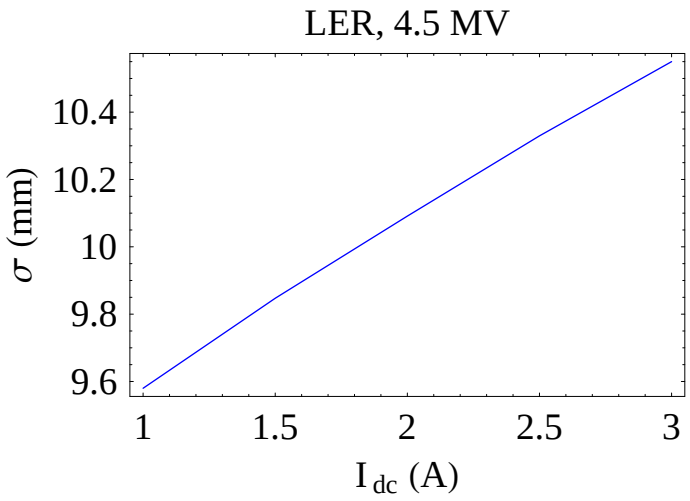

Figure 4: Averaged over the train bunch length vs beam current. Inductance $L = 80$ nH $d\sigma/dI_{dc} = 0.83$ mm/mA.

Another one depicts the calculated rms of a single bunch using measured frequency of synchrotron oscillations.

In Fig. (6) we show the measured synchrotron frequency ω_s of a bunch centroids as function of the beam current measured from the first and the second side-bands of the rf frequency. ω_s measured by the second method shows linear dependence on the beam current and deviate from the measurements by the first method due to effect of the feedback.

The few comments ought to be added. Generally, the bunch centroid motion is a superposition of harmonics of the CB frequencies, including the second harmonics $2\omega_{s,n}$. If the bunch-to-bunch frequency variation due to long gap transients is large, we can neglect bunch coupling caused by the longitudinal wake. In this case, all bunches have different frequencies and are approximately equal to $\omega_{s,n}$. The distribution of bunches over synchrotron frequencies calculated from the result depicted in the bottom plot of Fig. (2) for 1 Amp is shown in Fig. (7). It is similar to the actual profile of the side-band line in the spectrum observed in the LER. In the other extreme case, when the gap transients are small, the bunch frequencies are the frequencies of coupled-bunch modes and the set of these frequencies is the same for all bunches contrary to the shape of the spectrum for different bunches which still can be different because contributions of particular CB modes is not the same for different bunches.

For PEP-II LER, the spread of the CB modes is comparable with the variation of the synchrotron frequency along the train.

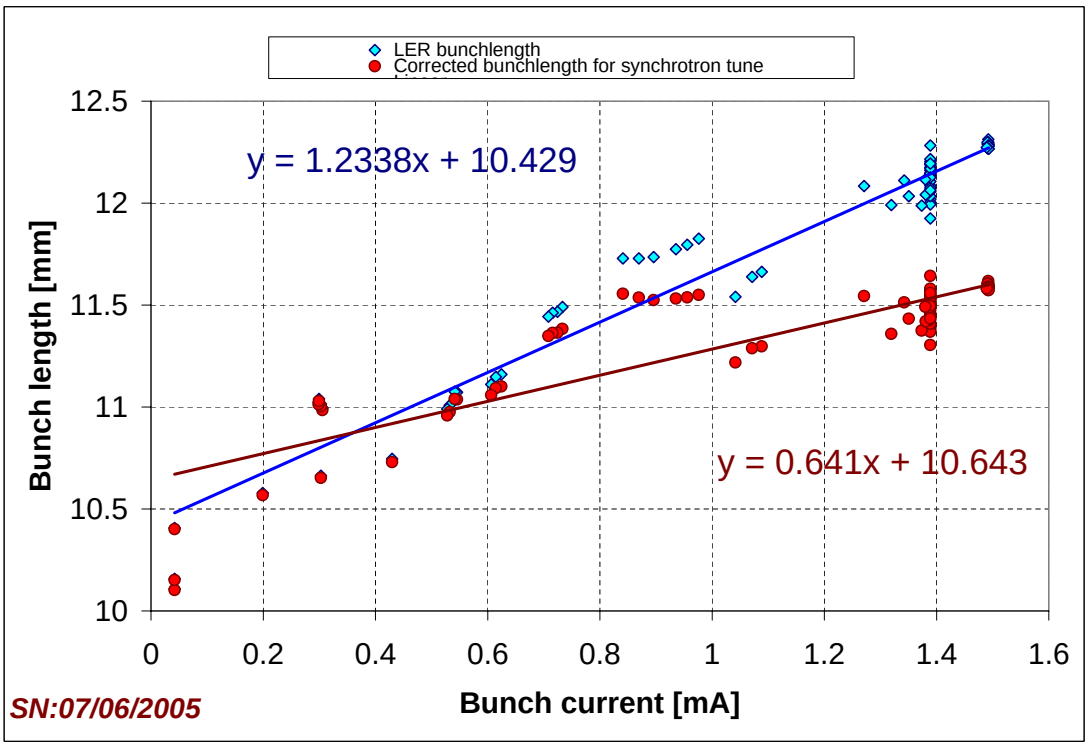

Figure 5: The measured bunch length in a train of bunches (blue) and the bunch length of a single bunch with the same rf voltage and bunch current calculated from the measured synchrotron tune.

2.2 Effect on luminosity

Variation of the synchronous phase affects luminosity of the collider in two ways. First, through the induced variation of the bunch length σ_l which, in its turn, changes luminosity L due to the hour-glass effect. Secondly, the waist of the bunch shifts longitudinally and collision takes place at the point with larger β-function and, therefore, with larger transverse rms. Effect is shown in Fig. (8). The upper plot shows the hour-glass effect: variation of the luminosity L_H/L_0 normalized by the nominal luminosity L_0 of the point-like bunches. The bottom plot shows additional drop of the luminosity L/L_H with the shift of the synchronous phase of one of bunches from the nominal phase. The luminosity is normalized on L_H. It is worth noting, that even if the rf phases of two beams are matched, the variation of the synchronous phase along the train remains and reduces the average luminosity. A special device such as dedicated harmonic cavity is needed to

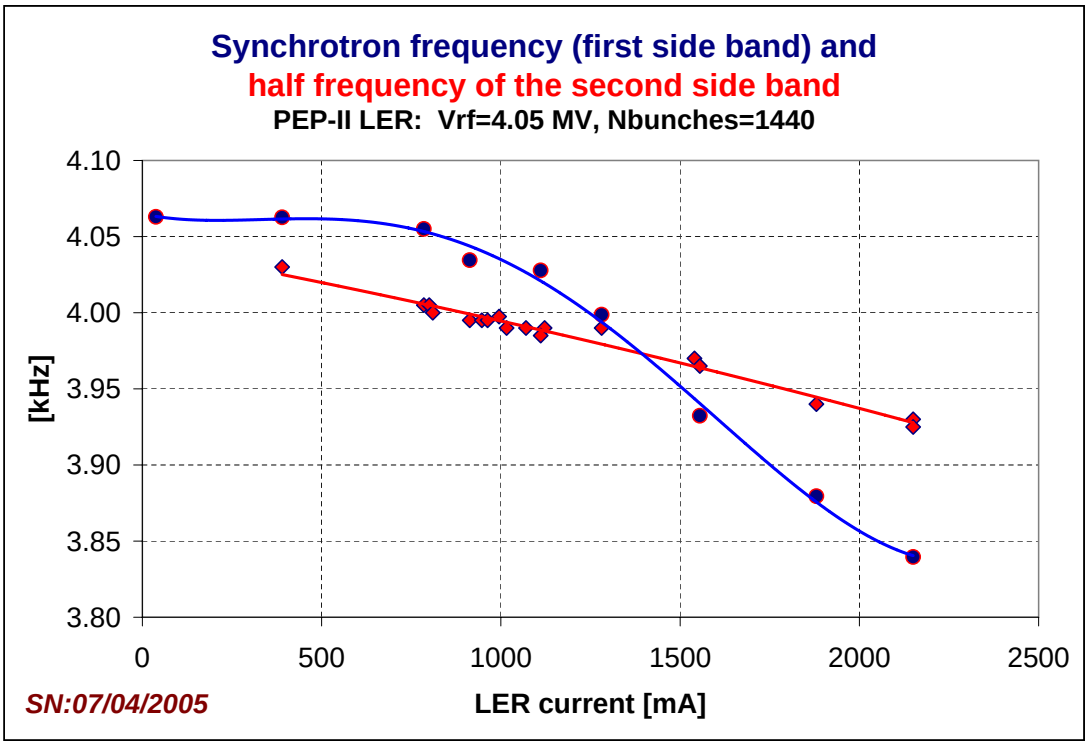

Figure 6: Synchrotron frequency measured from the first and the second side-bands in the beam spectrum.

eliminate this adverse effect.

It is worth noting that the synchronous phase variation can be more important at large crossing angles suggested for Super-B-factory [4].

Synchronous phase shift along the train can also be responsible for the variation of the tune along the train due to parasitic crossings.

3 Effect of the RW wake on tunes

As it is well known, the RW wake gives the dominant contribution to transverse dynamics, see Fig. (9),

Calculations of the corresponding tune variation of the transverse CB modes gives $\delta Q_x = 0.46\,10^{-2}$.

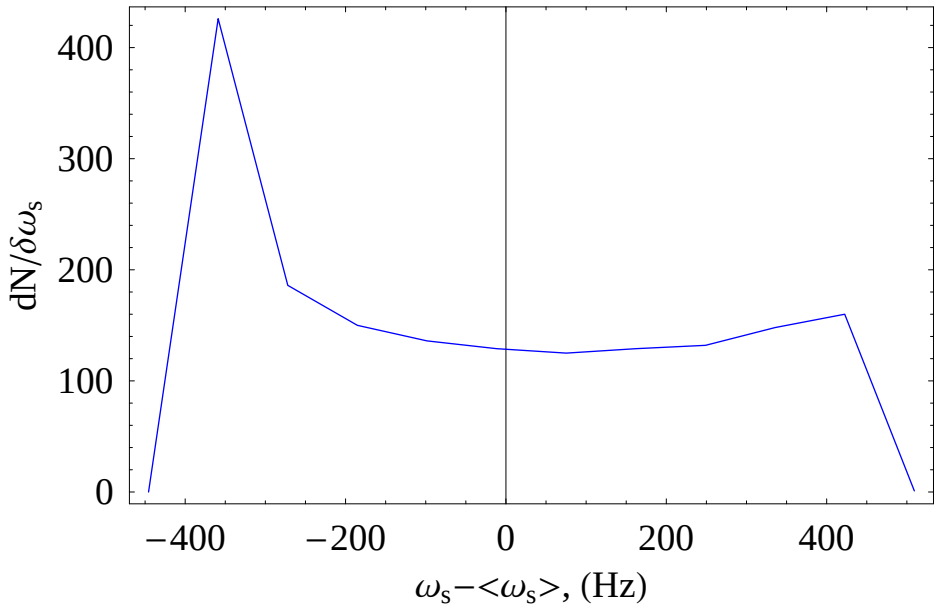

Figure 7: The shape of the synchrotron sideband in the case where transients give dominant effect, parameters for LER at 1 A current.

Experiment (A. Fisher, gated tune measurements) gives variation *along the train* of the same order monotonic for y-plane and oscillatory in x-plane.

This result deserves some comments. First of all, one can expect that all bunches are involved in n_B CB oscillations. Although the amplitudes of different modes for each bunch can be different, the CB frequencies should be the same for all bunches, even if the wake is substantially reduced across the gap. However, transients due to e-cloud, parasitic crossings at IP combined with the variation of the synchronous phase shift along the train, and the quadrupolar wake fields can cause the bunch-to-bunch tune variation. Actually, if such variation is larger that coupling between bunches, the CB modes are destroyed and bunches have different tunes.

For large gaps, the tune depends not only on the beam current but also on the number of bunches [6],

$$\frac{dQ_\perp}{dI_{beam}} \propto \frac{1}{n_b}\sqrt{\frac{R}{\sigma_B}} + \frac{\Gamma(1/4)}{\sqrt{1-Q_\perp}} + A, . \tag{5}$$

Here the 1st term is the single bunch effect, the second is multi-bunch effect, and the last term A is the effect of the beam pipe asymmetry. Effect of the first two terms is shown in Fig. (10). The calculation were carried out directly solving the system of CB equation for n-bunches coupled by the RW wake field.

The last term in Eq. (5) gives the dominant contribution for PEP-II. The very first

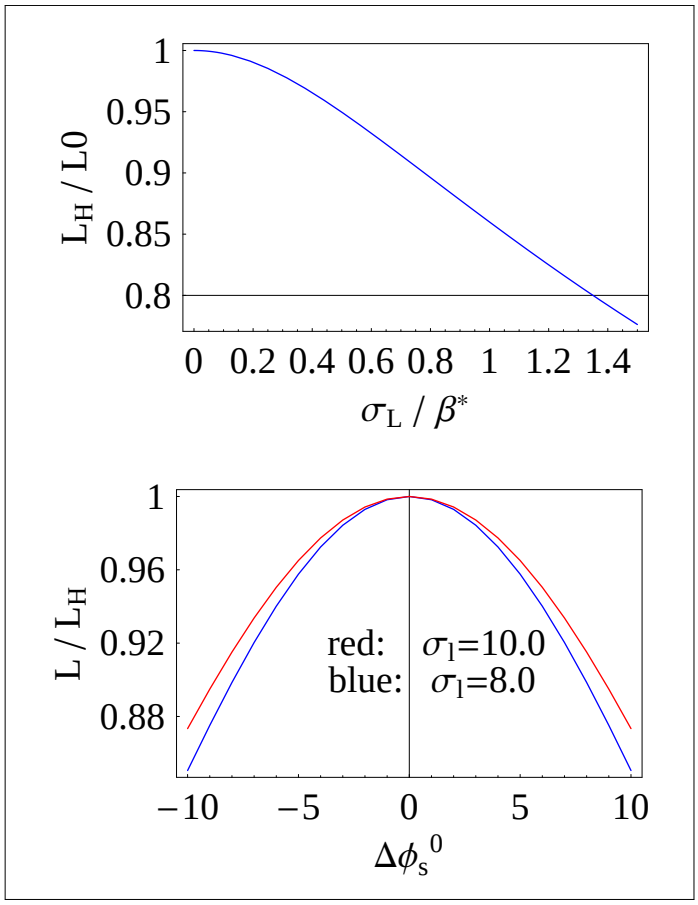

Figure 8: Hour-glass effect (left) and variation of the luminosity with the synchronous phase error (right) normalized to nominal L_0. $\beta_y^* = 1.0$ cm. a) hour-glass due to σ_l variation, b) gap transients due to syn. phase variation.

measurements of the tune dependence on current gave the opposite slope in x and y planes, see Fig. (11), while for the round beam pipe they have to be both negative. The effect has been explained [6, 7] as a result of the rectangular (more exactly, hexagonal) shape of the vacuum chamber in the arcs. The quadrupolar wake field in this case depends on offsets of both the leading and trailing particles. The part of the wakes of all $n_b \simeq 1700$ bunches proportional to the offset of the trailing bunch are add up and the amplitude of the resulting wake depends on the time of diffusion of the wake fields through the beam pipe wall. The typical build-up time is about 200 turns. This part does not exists for a round beam pipe. Result of calculation of the tune shift with current is shown in Fig. (12), where we compare the tune variation without quadrupolar wake (upper box) and with it (the box in the middle) with the experimental tune variation used for the forward

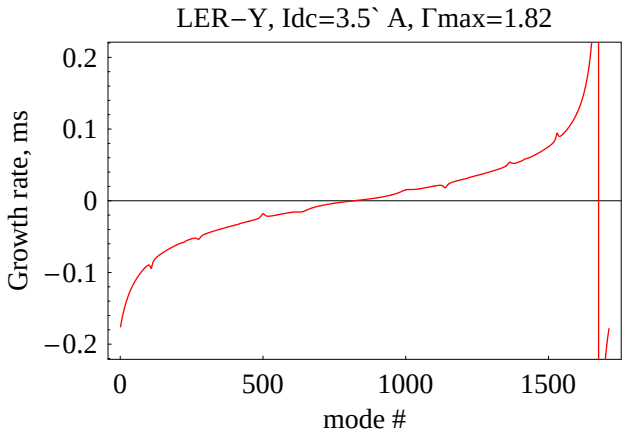

Figure 9: Growth rate vs CB mode number.

feedback in the control room. The calculation are based on real dimensions of the beam pipe but use 1D estimate of the diffusion time. We also give for comparison the single bunch tune shift [8] where the slope of $dQ_{x,y}/dI$ has the same sign in both planes.

3.1 Variation of the β-function and dispersion

Variation of the tune with current leads, of course, to the variation of the Twiss parameters. For illustration, effect was calculated using the code MAD for $Q_x = 38.518$. To simulate effect of the wake field on beam optics, we added a small ($K_1 \simeq 10{-}4$) quadrupole component to the main bends in the LER ring. This caused change of the tune by $\delta Q_x \simeq 10^{-3}$. One can expect such change of the tune with current due to wakes at I_b of couple amperes. The variation od the horizontal dispersion at IP, and the relative variation of the maximum of the beta-function and dispersion in the ring is given below:

$$\begin{aligned}
&\frac{dD_x^*}{dQ_x} = 4.\,10^{-2},\\
&\frac{1}{\beta_x^{max}}\,\frac{d\beta_x^{max}}{dQ_x} = 1.62,\\
&\frac{1}{D_x^{max}}\,\frac{dD_x^{max}}{dQ_x} = 0.15.
\end{aligned} \tag{6}$$

4 Conclusion

The optical effects of the wake fields are needed to explain some experimental observations. At large currents, their effect is not reduced to coherent instabilities. Wake can affect

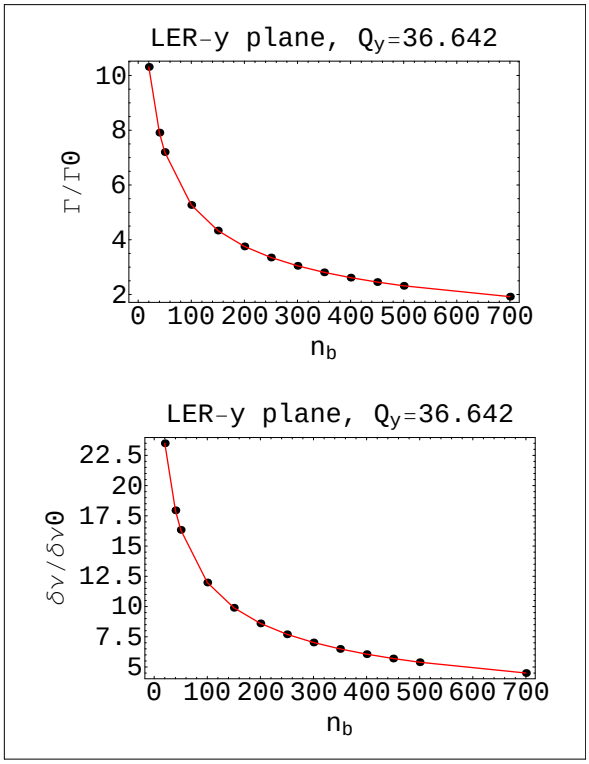

Figure 10: Growth rate and the tune shift as function of the number of bunches for a fixed beam current and bunch spacing.

the beam dynamics in the non-resonant way: it can change the tune, the synchronous phase, and the Twiss parameters along the train affecting the luminosity and optics of the collider. In particular, the effect of the variation of the synchronous phase along the train can be important for the design of Super-B-factory with large crossing angle.

5 Acknowledgement

We appreciate discussions with A. Chao and Y. Nosochkov.

Work supported by Department of Energy contract DE–AC03–76SF00515.

References

[1] A.W. Chao Physics of collective beam instabilities in high energy accelerators, J. Wiley and Sons, inc, 1993

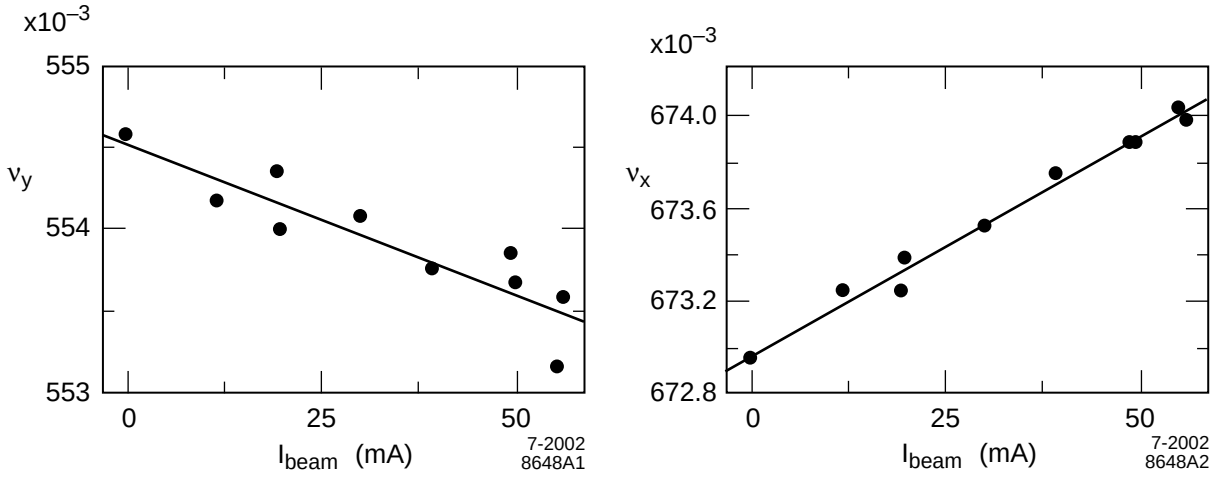

Figure 11: Measured tune variation with current

[2] D. Teytelman, Architectures and algorithms for control and diagnostics of coupled bunch instabilities in circular accelerators. Ph.D. Thesis, SLAC-R-633, June 2003.

[3] Super-B-factory Workshop, SLAC, June 2006.

[4] Towards Higher Luminosities in B and Phi Factories. P. Raimondi (Frascati) . EPAC-2004-FRXBCH02, Jul 2004. 4pp.

[5] S. Heifets, et. al., Impedance study of the PEP-II B-factory, SLAC/AP-99, March 1995.

[6] S. Heifets, Tune shift due to asymmetry of the resistive beam pipe, SLAC-PUB-7985, 1998.

[7] A. Chao, S. Heifets, B. Zotter, Tune shift of bunch trains due to resistive vacuum chambres without circular symmetry, PRST, 5, 111001, 2002.

[8] J. Turner, Private communication

6 Appendix: On the definition of the bunch length

We summarize here basic formulas used in our calculations.

We denote the distance of the center of the rf bucket occupied by the n-th bunch from the head of the train by S_n. In the case of equidistant bunches, $S_n = (n-1)s_b$, $n = 1, 2, ..n_b$, and $n = 1$ is the head of the train. The i-th particle of the n-th bunch on the k-th turn is located in the ring at the moment t at $ct - S_n - \zeta_n + z_{n,i} - kC$, where ζ_n

Without Quadrup. Field :

Theory : dν / dI, (1 / mA)	LER	HER
x	$-0.036\,10^{-5}$	$-0.015\ 10^{-5}$
y	$-0.103\ 10^{-5}$	$-0.041\ 10^{-5}$

With Quadrup. Field, Fe + Cu :

Theory : dν / dI, (1 / mA)	LER	HER
x	$1.62\,10^{-5}$	$0.80\ 10^{-5}$
y	$-1.41\ 10^{-5}$	$-2.45\ 10^{-5}$

Experiment :

Exper : dν / dI, (1 / mA)	LER	HER
x	$2.1\,10^{-5}$	$2.0\,10^{-5}$
y	$-1.5\,10^{-5}$	$-2.0\,10^{-5}$

Compare with LER single bunch (J. Turner) :

$d\nu_y$ / dI = -0.00226, (1 / mA)

$d\nu_x$ / dI = -0.00131, (1 / mA)

Figure 12: Results of the calculations with the model of the quadrupole wakes.

is related to the rf phase $\phi_n = \omega_{rf}\zeta_n/c$ of the n-th bunch, and $z_{n,k}$ is the shift of particles from the bunch center. The shift is positive for offset toward the head of the train.

The longitudinal motion is described by a Hamiltonian $H = \sum H_m(p_{m,i}, z_{m,i}, s)$, where the canonical momentum $p_{m,i} = -\alpha\delta_{m,i}$ is defined in terms of the momentum compaction α and the energy shift $\delta = (E - E_0)/E_0$, and

$$H_n = \frac{p_{n,i}^2}{2} + (\frac{\omega_{s,0}}{c})^2\,\frac{z_{n,i}^2}{2} + \frac{\alpha}{E_0 C}\,[eV_{rf}\cos[\phi_n] - U_l]\,z_{n,i} + \int dz'\rho_n(z',s)G[z' - z_{n,i}]$$
$$+\lambda\sum_{m,k}\int dz'\rho_m(z',s)G[z' - z_{n,i} + S_n - S_m + kC]. \qquad (7)$$

Here

$$\lambda = \frac{\alpha N_B e^2}{E_0 C} \qquad (8)$$

and we neglected the nonlinearities of the rf potential. Other notations are standard: V_{rf} is the rf voltage per turn, $\omega_{rf} = h\omega_0$, $\omega_0 = 2\pi c/C$, U_l is the SR energy loss per

turn per particle, $C = 2\pi R$ is circumference, N_B is bunch population. The dimensionless function $G(z)$ is given by the two-particle longitudinal wake $W(z)$, $G(z) = \int_0^z dz' W(z')$, and prime in $W'(z)$ means the derivative over the argument. Note that $G(z) = 0$ for $z < 0$, and $W(z) > 0$ corresponds to the energy loss. The sum in Eq. (12) is over all bunches in the train preceding the bunch n including previous turns. Finally, ω_{s0} is the zero-current synchrotron frequency ω_{s0},

$$(\frac{\omega_{s,0}}{\omega_0})^2 = \frac{\alpha e h V r f}{2\pi E_0} \sin\phi_n. \tag{9}$$

For a bunch current below the threshold of the microwave instability, the density of the n-th bunch in the phase plane can be written as $F_n(z, p, s) = F_n(z - Z_n(s), p)$ where $Z_n(s)$ describes oscillations of the bunch center. The bunch density ρ_n then is

$$\rho_n(z, s) = \int dp F_n(z, p, s) = \rho_n(z - Z(s)), \quad \int dz \rho_n(z, s) = 1. \tag{10}$$

It is convenient to use canonical variables $\hat{z}_{n,i}$, $\hat{p}_{n,i}$ describing motion in the frame oscillating with the bunch center,

$$z_{n,i} = Z_n(s) + \hat{z}_{n,i}, \quad p_{n,i} = Z_n'(s) + \hat{p}_{n,i}. \tag{11}$$

The centroid trajectory $Z_n(s)$ is defined below.

The canonical transform to new variables can be done with the generating function $\Phi(\hat{p}, z, s) = (z - Z_n)\hat{p} + Z'(s)z$, where $Z_n' = dZ_n(s)/ds$. The new Hamiltonian $\hat{H}(\hat{z}_{ni}, \hat{p}_{ni}) = H + \partial\Phi/\partial s$ takes the form

$$\begin{aligned}
&\hat{H}_n(\hat{z}, \hat{p}) = \frac{\hat{p}^2}{2} + (\frac{\omega_{s,0}}{c})^2 \frac{\hat{z}^2}{2} + (\frac{\omega_{s,0}}{c})^2 \hat{z} Z_n(s) + \frac{\alpha}{E_0 C} \left[eV_{rf} \cos[\phi_n] - U_l\right] \hat{z} \\
&+ Z_n''(s)\hat{z} + \int dz' \rho_n(z') G[z' - \hat{z}] \\
&+ \lambda \sum_{m,k} \int dz' \rho_m(z') G[kC + S_n - S_m + Z_m(s - kC) - Z_n(s) + z' - \hat{z}].
\end{aligned} \tag{12}$$

Expanding the last term over $Z_m(s - kC) - Z_n(s) + z' - \hat{z}_{n,i} << s_b$ and omitting terms independent of the canonical variables, we get

$$\hat{H}_n(\hat{z}, \hat{p}) = \frac{\hat{p}^2}{2} + (\frac{\hat{\omega}_s}{c})^2 \frac{\hat{z}^2}{2} + \int dz' \rho_n(z') G[z' - \hat{z}] + \lambda z \int dz' dz'' \rho_n(z') \rho_n(z'') G(z' - z''). \tag{13}$$

Here we used the definition of the bunch center $\int dz \rho_n(z) z = 0$, notations

$$(\frac{\hat{\omega}_s}{c})^2 = (\frac{\omega_{s,0}}{c})^2 + \lambda \sum_{m,k} W'[kC + S_n - S_m], \tag{14}$$

equation for the rf phase

$$eV_{rf}\cos[\phi_n] = U_l + N_B e^2 \sum_{k,m} W[kC + S_n - S_m] + N_B e^2 \int dz dz' \rho_n(z)\rho_n(z')G(z'-z), \quad (15)$$

and define $Z_n(s)$ as a solution of the coupled-bunch equations

$$Z_n''(s) + (\frac{\hat{\omega}_s}{c})^2 Z_n(s) = \lambda \sum_{m,k} W'[kC + S_n - S_m] Z_m(s - kC). \quad (16)$$

Here the sum is over turns $k = 0, 1, ..$ and over all M bunches in the ring $m = 1, 2.., M$ for $k \neq 0$ and for $m = 1, 2.., n-1$ for $k = 0$.

The rf phase ϕ_n is defined in Eq. (15) by the total energy loss per turn. Note that the average contribution of the fundamental rf mode wake should not be included in Eq. (15) because it is already taken into account as the beam loading contribution to the rf voltage.

For a non-uniform fill, the rf phases of different bunches are different. The transients effect is mostly given by fundamental mode of the rf cavities. Variation of ϕ_n along the train of bunches changes frequencies ω_{s0}, see Eq. (9), affecting $\hat{\omega}_s$ of individual bunches additional to the effect of the wake of the last term in Eq. (14).

Eqs. (14)-(15) define frequencies of oscillations of bunch centers.

For the uniform distribution of the bunches around the ring, solution of Eq. (16) is given as a superposition of eigen modes with the amplitudes a_μ

$$Z_n(s) = \sum_{\mu=0}^{M} a_\mu X_n^\mu \, e^{-i\frac{\Omega_\mu}{c}[s+(n-1)s_b]}, \quad X_n^\mu = \frac{1}{\sqrt{M}} e^{2\pi i \frac{(n-1)\mu}{M}}. \quad (17)$$

where frequencies are given in terms of the longitudinal impedance per turn $Z(\omega)$,

$$\Omega_\mu^2 - \omega_{s0}^2 = i\lambda M \frac{\omega_0^2}{2\pi} \sum_p \{(pM + \mu + \frac{\Omega_\mu}{\omega_0}) Z[(pM + \mu + \frac{\Omega_\mu}{\omega_0})\omega_0] - pMZ[pM\omega_0]\} e^{-(pM+\mu+\Omega_\mu/\omega_0)^2(\frac{2\pi\sigma_0}{C})^2}. \quad (18)$$

The Fokker-Plank equation with the Hamiltonian Eq. (13) has the steady-state Haissinski solution

$$F(\hat{p}, \hat{z}) = \frac{1}{|N|} e^{-\frac{H_n}{T}}, \quad (19)$$

where $|N|$ is a normalization constant, and $\rho_n(\hat{z}) = \int dp F(\hat{p}, \hat{z})$. The temperature T should be defined to give the rms energy spread δ_0^2. Hence, $\langle p^2 \rangle = T = (\alpha\delta_0)^2$.

For currents below threshold of the microwave instability, parameter

$$\Lambda = \frac{\lambda}{T} = \frac{N_B e^2}{E_0 C \alpha \delta_0^2} \quad (20)$$

is small. In the linear approximation,

$$\rho_n(\hat{z}) = \frac{1}{|N|}\, e^{-(\frac{\hat{\omega}_s}{c})^2 \frac{\hat{z}^2}{2}} \{1 + \Lambda \int dz' \rho_n(z') G[z' - \hat{z}] + \Lambda \hat{z} \int dz' dz'' \rho_n(z') \rho_n(z'') G(z' - z'')\}. \tag{21}$$

The normalization constant $|N|$ is defined by the condition $\int dz \rho_n(z) = 1$. It is easy to check that the average $\langle z \rangle = \int dz z \rho(z) = 0$. Simple calculations give the rms bunch length σ,

$$\begin{aligned} \sigma^2 &= \int dz z^2 \rho_n(z), \\ \sigma^2 &= \sigma_0^2 (\frac{\omega_{s0}}{\hat{\omega}_s})^2 \{1 - \frac{\Lambda}{2\sqrt{2\pi}} \int dx G[\frac{\omega_{s0}}{\hat{\omega}_s} \sqrt{2} \sigma_0 x]\, [1 - x^2]\, e^{-\frac{x^2}{2}}\} + o(\lambda^2). \end{aligned} \tag{22}$$

In the linear approximation over Λ, $\omega_{s0}/\hat{\omega}_s$ in the argument of G can be replaced by one.

The frequency Eq. (14) includes the effect of the long-range wake field. If the multi-turn wake can be neglected, then for a single bunch $\hat{\omega}_s = \omega_{s0}$, and the single bunch rms σ_1 is

$$\sigma_1^2 = \sigma_0^2 \{1 - \frac{\Lambda}{2\sqrt{2\pi}} \int dx G[\sqrt{2} \sigma_0 x]\, [1 - x^2]\, e^{-\frac{x^2}{2}} + o(\lambda^2). \tag{23}$$

Eqs. (22),(23) show that in the linear approximation over the bunch current the rms of a bunch in a train and of a single bunch are different,

$$\sigma_1^2 = (\frac{\hat{\omega}_s}{\omega_{s,0}})^2 \sigma^2. \tag{24}$$

The difference is due to the long-range wake.

As an example we calculated the CB frequencies for LER of PEP-II using our model of the LER PEP-II machine impedance and Eq. (18). The frequencies of the dipole CB modes can be written as

$$\begin{aligned} \Omega_\mu^D &= \hat{\omega}_s + \frac{d\Omega_\mu^D}{dI} I_{beam}, \\ \hat{\omega}_s &= \omega_{s0} - \frac{d\Omega_0}{dI} I_{beam}, \end{aligned} \tag{25}$$

where the slopes for the dipole CB longitudinal modes are:

$$\frac{d\Omega_\mu^D}{dI} = Re\{i\frac{\alpha\omega_0^2}{4\pi\omega_{s0}E_0/e}\sum_p (pM+\mu)Z[(pM+\mu)\omega_0]\},$$
$$\frac{d\Omega_0}{dI} = i\frac{\alpha\omega_0^2}{4\pi\omega_{s0}E_0/e}\sum_p pM\, Z[pM]. \tag{26}$$

Calculations (see Fig. (13)) give

$$\langle\frac{d\Omega_\mu^D}{dI}\rangle = 1410\,(\frac{\mathrm{Hz}}{\mathrm{A}}), \quad \frac{d\Omega_0}{dI} = 1417\,(\frac{\mathrm{Hz}}{\mathrm{A}}). \tag{27}$$

Two terms in Ω_μ almost cancel in agreement with Fig.6 at low currents. At high current the slope depends on the feedback and the nolinear terms $o(I^2)$.

For the quadrupole modes the calculated slope of different modes is small and about constant for all modes,

$$\Omega_\mu^Q = 2\hat{\omega}_s + \frac{d\Omega_\mu^Q}{dI}\, I_{beam},$$
$$\frac{d\Omega_\mu^Q}{dI} \simeq 246\,(\frac{\mathrm{Hz}}{\mathrm{A}}). \tag{28}$$

Therefore, the slope of Ω_μ^Q is given with good accuracy by the first term $2\hat{\omega}_s$ what allows to define $\hat{\omega}_s$ from measurements of the slope of the second side-band in the beam spectrum.

With known $\frac{d\Omega_0}{dI}$, we can derive the rms length of a single bunch from measurements of the average bunch length $\sigma = \sigma_0 + (d\sigma/dI)I_{beam}$ in the train of bunches using Eq. (29):

$$\sigma_1 = (1 - \frac{1}{\omega_{s0}}\frac{d\Omega_0}{dI}I_{beam})\,(\sigma_0 + \frac{d\sigma}{dI}\, I_{bunch}) \simeq \sigma_0 + I_{bunch}(\frac{d\sigma}{dI} - M\frac{d\Omega_0}{dI}\frac{\sigma_0}{\omega_{s0}}). \tag{29}$$

Fig. 5 gives $\sigma_0 = 10.6$ mm and $d\sigma/dI_{bunch} = 1.2$ mm/mA. Correction with calculated $\frac{d\Omega_0}{dI}$, $\omega_{s0} = 26.7$ kHz, and $M = 1722$ is large, $M(d\Omega_0/dI)(\sigma_0/\omega_{s0}) \simeq 0.9$. Experimental slope of $\hat{\omega}_s$ is smaller, $d\Omega_0/dI \simeq 400$, see Fig. 6, and the correction $M(d\Omega_0/dI)(\sigma_0/\omega_{s0}) \simeq 0.27$.

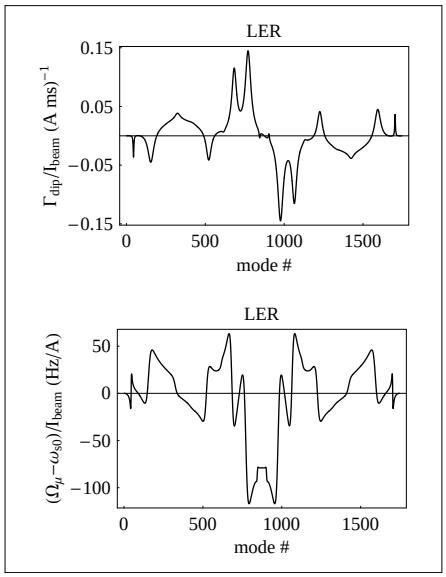

Figure 13: CB longitudinal dipole modes.